Stable Dilute Supersolid of Two-Dimensional Dipolar Bosons

Zhen-Kai Lu,[1] Yun Li,[2] D. S. Petrov,[3] and G. V. Shlyapnikov[3,4,5,6]
[1]Max-Planck-Institut für Quantenoptik, Hans-Kopfermann-Straße 1, 85748 Garching, Germany
[2]Centre for Quantum and Optical Science, Swinburne University of Technology, Melbourne, Victoria 3122, Australia
[3]Université Paris-Sud, CNRS, LPTMS, UMR8626, Orsay F-91405, France
[4]Van der Waals-Zeeman Institute, University of Amsterdam, Science Park 904, 1098 XH Amsterdam, The Netherlands
[5]Russian Quantum Center, Novaya Street 100, Skolkovo, Moscow Region 143025, Russia
[6]Wuhan Institute of Physics and Mathematics, Chinese Academy of Sciences, Wuhan 430071, China
(Received 3 October 2014; revised manuscript received 5 June 2015; published 14 August 2015)

We consider two-dimensional bosonic dipoles oriented perpendicularly to the plane. On top of the usual two-body contact and long-range dipolar interactions we add a contact three-body repulsion as expected, in particular, for dipoles in the bilayer geometry with tunneling. The three-body repulsion is crucial for stabilizing the system, and we show that our model allows for stable continuous space supersolid states in the dilute regime and calculate the zero-temperature phase diagram.

DOI: 10.1103/PhysRevLett.115.075303 PACS numbers: 67.80.K-, 03.75.Hh, 05.30.Rt, 67.85.-d

Recent advances in the field of cold polar molecules [1,2] and magnetic atoms [3,4] interacting via long-range dipole-dipole forces make it realistic to create novel many-body quantum states in these systems. For polar molecules, ultracold chemical reactions observed at JILA [5,6] and leading to a rapid decay of the system can be suppressed by tightly confining the molecules to a (quasi-)two-dimensional (2D) geometry, orienting the dipoles perpendicularly to the plane of their translational motion, and thus inducing a strong intermolecular repulsion [7–9]. Therefore, 2D geometries are intensively discussed in the context of ultracold dipolar gases [10–13], together with possible experiments with nonreactive molecules such as NaK [14,15] and RbCs [16,17].

The studies of ultracold dipolar gases may open perspectives for the observation of supersolidity. This remarkable quantum phenomenon combines superfluidity with a crystalline order [18,19] (see Ref. [20] for review). It is still under debate as to what extent experimental results in solid helium prove the existence of this conceptually important phase [21]. On the other hand, supersolidity is rather well understood theoretically for soft-core two-body potentials [20,22–26], which can be realized, for example, in Rydberg-dressed atomic gases. However, such supersolids require a dense regime with at least several particles within the interaction range, which can be difficult to achieve. The same holds for supersolids discussed for 2D dipolar Bose gases [27] near the gas-solid phase transition [28,29]. It is thus an open question whether supersolids can exist in the dilute regime. The creation of such supersolids, especially if they are tunable regarding the lattice period, will allow for studies of nonconventional superfluid properties of supersolids and other aspects of supersolidity. Dilute 2D dipolar bosons may show the (heliumlike) roton-maxon structure of the spectrum by fine tuning the short-range part of the interaction potential and can be made unstable with respect to periodic modulations of the order parameter (roton instability) [30]. However, instead of forming a supersolid state when approaching such an instability, the gas collapses [31,32].

In this Letter we predict a stable supersolid state in a dilute two-dimensional dipolar system. In contrast to the earlier proposed soft-core supersolids, where the lattice period is of the order of the core radius, in our case it is tunable by varying the density and the dipole moment. In addition to the contact two-body term g_2 and the dipole-dipole long-range tail characterized by the dipole moment d, we include a contact repulsive three-body term g_3, which may prevent the collapse. Three-body forces are ubiquitous and arise naturally in effective field theories when one integrates out some of the high-energy degrees of freedom in the system [33]. In particular, our model can be realized for dipoles in the bilayer geometry with interlayer tunneling [34]. Tracing out the degree of freedom associated with the layer index one obtains an effective single-layer model in which g_2 and g_3 can be independently controlled by tuning the interlayer tunneling amplitude. Here, we work out the phase diagram of this model and identify stable uniform and supersolid states.

The Hamiltonian of the system reads

$$\mathcal{H} = -\int d^2 r \hat{\psi}^\dagger(\mathbf{r}) \frac{\hbar^2 \nabla^2}{2m} \hat{\psi}(\mathbf{r}) + \mathcal{H}_2 + \frac{g_3}{6} \int d^2 r \hat{\psi}^\dagger(\mathbf{r}) \hat{\psi}^\dagger(\mathbf{r}) \hat{\psi}^\dagger(\mathbf{r}) \hat{\psi}(\mathbf{r}) \hat{\psi}(\mathbf{r}) \hat{\psi}(\mathbf{r}), \quad (1)$$

where $\hat{\psi}(\mathbf{r})$ is the bosonic field operator, m is the particle mass, and the normalization volume is set equal to unity. The first term in Eq. (1) corresponds to the kinetic energy, the third one to the contact three-body repulsion ($g_3 > 0$), and the two-body interaction Hamiltonian $\mathcal{H}_2$ at low energies can be substituted by an effective momentum-dependent (pseudo)potential (see, e.g., Ref. [35])

$$\tilde{V}(\mathbf{k},\mathbf{k}') = \tilde{V}(|\mathbf{k}-\mathbf{k}'|) = g_2 - 2\pi d^2|\mathbf{k}-\mathbf{k}'|, \quad (2)$$

where $\mathbf{k}$ and $\mathbf{k}'$ are the incoming and outgoing relative momenta, g_2 is the contact term, which depends on the short-range details of the two-body potential, and the momentum-dependent part corresponds to the long-range dipolar tail for dipoles oriented perpendicularly to the plane of their translational motion. We thus have

$$\mathcal{H}_2 = \frac{1}{2}\int d^2r d^2r' \hat{\psi}^\dagger(\mathbf{r})\hat{\psi}^\dagger(r')\sum_{\mathbf{q}} \tilde{V}(q)e^{i\mathbf{q}(\mathbf{r}'-\mathbf{r})}\hat{\psi}(\mathbf{r})\hat{\psi}(r'). \quad (3)$$

The onset of supersolidity is frequently associated with the presence of a low-lying roton minimum in the excitation spectrum [23,36,37]. In our case the standard Bogoliubov approach for a uniform Bose condensate of density n gives the excitation spectrum

$$\epsilon(k) = \sqrt{E_k^2 + 2E_k(g_2 n + g_3 n^2 - 2\pi n d^2 k)}, \quad (4)$$

where $E_k = \hbar^2 k^2/2m$, and we assume that $(g_2 + g_3 n) > 0$. The validity conditions for the mean-field approach read

$$nr_*^2 \ll 1, \qquad m(g_2 + g_3 n)/\hbar^2 \ll 1, \quad (5)$$

where $r_* = md^2/\hbar^2$ is a characteristic range of the dipole-dipole interaction. The structure of the spectrum is characterized by a dimensionless parameter β given by

$$\beta = \gamma/(1 + g_2/g_3 n), \qquad \gamma = 4\pi^2\hbar^2 r_*^2/m g_3. \quad (6)$$

The excitation energy $\epsilon(k)$ shows a roton-maxon structure (local maximum and minimum at finite k) for β in the interval $8/9 < \beta < 1$, and at $\beta = 1$ the roton minimum touches zero. For $\beta > 1$ the excitation energies become imaginary, and the uniform superfluid (U) is dynamically unstable and is no longer the ground state.

A promising candidate for the new ground state is a supersolid state in which the condensate wave function is a superposition of a constant term and a lattice-type function of coordinates [18,19,23,36]. We considered various lattice structures and found that the ground state can be either a triangular lattice supersolid (T) or a stripe supersolid (S) [38]. For the T phase, the lattice is built up on three vectors in the x, y plane of the translational motion, with the angle of $2\pi/3$ between each pair: $\mathbf{k_1} = (k, 0)$, $\mathbf{k_2} = (-k/2, \sqrt{3}k/2)$, and $\mathbf{k_3} = (-k/2, -\sqrt{3}k/2)$, while for the S phase the density modulation depends only on one wave vector $\mathbf{k} = (k, 0)$.

The variational *Ansatz* for the condensate wave function of the T phase then takes the form

$$\psi_T(\mathbf{r}) = \sqrt{n}\left(\cos\theta + \sqrt{2/3}\sin\theta e^{i\Phi}\sum_i \cos\mathbf{k}_i\mathbf{r}\right), \quad (7)$$

and for the S phase we have

$$\psi_S(\mathbf{r}) = \sqrt{n}(\cos\theta + \sqrt{2}\sin\theta e^{i\Phi}\cos kx), \quad (8)$$

which satisfies the normalization condition $\int d\mathbf{r}|\psi_{T(S)}(\mathbf{r})|^2 = n$, with n being the mean density. The variational parameters of the wave functions are θ, Φ, and k. Density modulations appear at $\theta \neq 0$, and thus θ is the order parameter that exhibits the U to supersolid transition. We have checked that the lowest energy always corresponds to $\Phi = 0$ and for brevity we omit this parameter.

For obtaining the energy functionals of the T and S states, we replace the field operators in Eqs. (1) and (3) with $\psi_T(\mathbf{r})$ and with $\psi_S(\mathbf{r})$, respectively. This yields

$$\mathcal{E}_i = [E_k n - 4\pi n^2 d^2 k \mathcal{D}_i(\theta)]\sin^2\theta + g_2 n^2 \mathcal{C}_i(\theta) + g_3 n^3 \mathcal{T}_i(\theta), \quad (9)$$

where the symbol i stands for T and S, and the functions $\mathcal{D}_{T(S)}(\theta)$, $\mathcal{C}_{T(S)}(\theta)$, and $\mathcal{T}_{T(S)}(\theta)$ are related to the two-body dipole-dipole, two-body contact, and three-body contact interactions, respectively [38].

By minimizing Eq. (9) with respect to k we obtain

$$\mathcal{E}_i(k_{mi}) = g_2 n^2 \mathcal{C}_i(\theta) + g_3 n^3[\mathcal{T}_i(\theta) - 2\gamma\sin^2\theta\mathcal{D}_i^2(\theta)], \quad (10)$$

where $k_{mi} = 4\pi n r_* \mathcal{D}_i(\theta)$. In the dilute limit of Eq. (5) the particle number per unit modulation volume is $n(2\pi/k_{mi})^2 \sim 1/nr_*^2 \gg 1$, which justifies the mean-field approach.

The energy functional $\mathcal{E}_{T(S)}$ can be expanded in powers of θ. The zero-order term $\mathcal{E}(\theta = 0) = g_2 n^2/2 + g_3 n^3/6$ gives the energy density of the uniform state. The expansion of $\mathcal{E}_T$ contains terms $\propto \theta^3$ [38], which is a consequence of the fact that the vectors $\mathbf{k}_1$, $\mathbf{k}_2$, and $\mathbf{k}_3$ form a closed triangle ("triad," $\mathbf{k}_1 + \mathbf{k}_2 + \mathbf{k}_3 = 0$) [19]. In contrast, the expansion of $\mathcal{E}_S$ contains only even powers of θ. According to the Ginzburg-Landau theory [41,42], the U-supersolid transition should occur to the T phase and it is expected to be first order, so that θ jumps from 0 to a finite value. However, deeply in the supersolid regime the states with different structures are energetically competing and, in particular, the stripe phase can become the ground state of the system.

First-order transitions are convenient to analyse in the grand-canonical picture. We obtain the phase diagram by variationally minimizing the grand potential $\Omega = \mathcal{E}_{T(S)} - \mu n$ with respect to θ and n for given values of the chemical potential μ and the interaction parameters g_2, g_3, and d. We have checked the phase diagram by employing the full numerical minimization of the grand potential density, which is equivalent to solving the corresponding Gross-Pitaevskii (GP) equation [38].

First, let us consider $g_2 = 0$. In this case the energy functional $\mathcal{E}$ only contains terms $\propto n^3$, and the phase

diagram is determined by a single dimensionless parameter γ defined in Eq. (6). The U to T transition occurs before the roton minimum touches zero (for $g_2 = 0$ we have $\beta = \gamma$), namely, at $\gamma_0 \simeq 0.99$, where θ jumps from 0 to 0.0946. The inverse compressibility $\kappa^{-1} = \partial\mu/\partial n = 6\mathcal{E}/n^2$ is positive for γ smaller than approximately 1.4, indicating the existence of a stable supersolid state. However, our numerics predicts the collapse instability at about $\gamma_c \approx 0.88$ and indicates that for lower values of γ the ground state is a uniform superfluid. The discrepancy between the numerics and the variational *Ansatz* comes from the fact that the latter does not take into account higher order momentum harmonics.

For $g_2 \neq 0$, we turn to the rescaled dimensionless density $\tilde{n} = ng_3/|g_2|$, chemical potential $\tilde{\mu} = \mu g_3/g_2^2$, and grand potential $\tilde{\Omega}_{T(S)} = (g_3^2/|g_2|^3)\Omega_{T(S)} = \tilde{E}_{T(S)} - \tilde{\mu}\tilde{n}$. The rescaled energy functional is given by

$$\tilde{E}_i = [\mathcal{T}_i(\theta) - 2\gamma\sin^2\theta\mathcal{D}_i^2(\theta)]\tilde{n}^3 + \mathrm{sgn}(g_2)\tilde{n}^2\mathcal{C}_i(\theta). \quad (11)$$

The phase diagram can be presented in the parameter space $(\tilde{\mu}, \gamma)$ and the phases are characterized by $\theta \in [-\pi/2, \pi/2]$ and $\tilde{n}$. One can easily see that in the high-density regime $\tilde{\Omega}_{T(S)}$ is dominated by the term $[\mathcal{T}_{T(S)}(\theta) - 2\gamma\sin^2\theta\mathcal{D}_{T(S)}^2(\theta)]\tilde{n}^3$, whereas the two-body contact interaction, i.e., the term containing $\mathcal{C}_{T(S)}(\theta)$, becomes irrelevant [43]. In this case the T phase has a lower $\tilde{\Omega}$ than the S phase, and we obtain the same stability condition as in the case of $g_2 = 0$. Numerically, we find that the phase diagram for $g_2 > 0$ contains only a stable U state at $\gamma < \gamma_c$ and the region of collapse for $\gamma > \gamma_c$.

The situation is quite different for $g_2 < 0$. The phase diagram is shown in Fig. 1 where all continuous curves correspond to the variational results and all symbols to the exact numerical solution of the GP equation. Let us first discuss the variational results. The dashed curves mark the U-$T_{\theta<0}$ and U-$T_{\theta>0}$ transitions, which occur for $\tilde{\mu} < 3/2$ and $\tilde{\mu} > 3/2$, respectively. These are first-order transitions, which weaken on approaching the point $\tilde{\mu} = 3/2, \gamma = 2/3$ (black dot). The same holds for the dotted curves, which correspond to the transitions from the T phases to the S phase. The black dot thus stands as a four-critical point and it is the only place in the phase diagram where the transitions are second order and occur when the roton minimum touches zero. In this case the grand potential $\tilde{\Omega} = \mathrm{const} + O(\theta^4)$; i.e., the terms $\propto \theta^2$ and $\propto \theta^3$ are absent.

The region on the left of the black solid curve in Fig. 1 is the vacuum state: $\tilde{n} = 0, \Omega = 0$. Directly on the curve, vacuum can coexist with matter that has a finite density and zero pressure. We thus are dealing with a self-trapped droplet state [44]. With increasing γ, the vacuum curve eventually bends towards negative $\tilde{\mu}$ and tends to the variational collapse line $\gamma \approx 1.4$ (not shown).

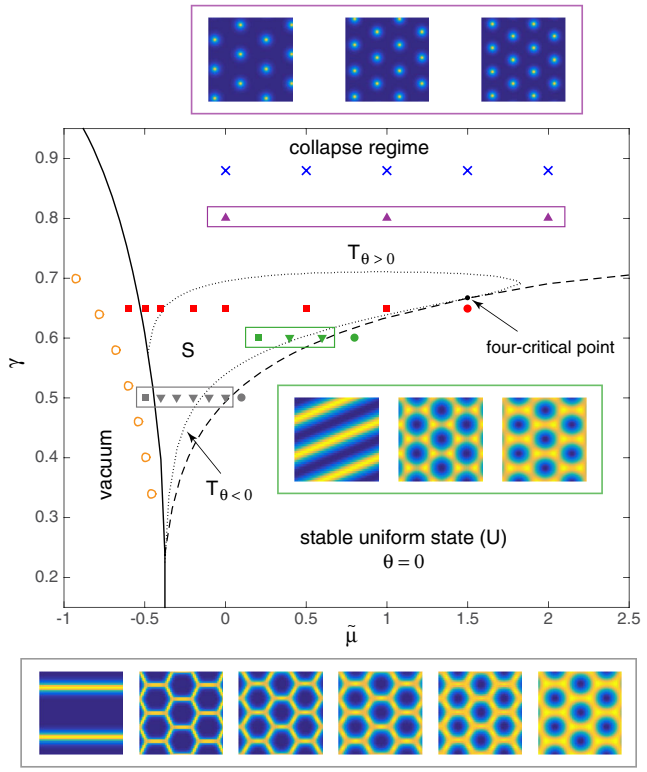

FIG. 1 (color online). Phase diagram for $g_2 < 0$. Continuous curves correspond to transitions between different phases obtained from the variational *Ansätze* (7) and (8). Increasing γ one passes the U-T transition (dashed), then the T-S transition (lower dotted curve), and the S-T transition (upper dotted curve). To the left of the solid black curve the ground state of the system is vacuum. The black dot is the four-critical point for the U, S, and two T phases. The symbols indicate our numerical results: the filled circles are inside the U phase, the downward and upward pointing triangles are inside the $T_{\theta<0}$ and $T_{\theta>0}$ phases, respectively, and the squares are in the stripe phase. The empty circles are on the vacuum-stripe line and the crosses are at the collapse instability border. The color-coded pictures show density profiles corresponding to the symbols in the phase diagram put in frames: the upper set (violet frame) contains three points of the $T_{\theta>0}$ phase at $\gamma = 0.8$, the middle set (green frame) shows one point in the S phase and two points in the hexagonal $T_{\theta<0}$ phase at $\gamma = 0.6$, and the lower set (gray frame) corresponds to the six points at $\gamma = 0.5$.

By solving the GP equation numerically we observe that the overall structure of the phase diagram is well captured by the variational *Ansätze* (7) and (8). Close to the four-critical point the agreement is quantitative, which is generally expected in the regions where $\theta \ll 1$. Far from this point we see that the exact collapse line moves to $\gamma \approx 0.88$ (crosses in Fig. 1) and the vacuum curve (empty orange circles) bends towards negative $\tilde{\mu}$ faster than its variational version. The rest of the symbols in Fig. 1 are inside the U phase (filled circles), $T_{\theta<0}$ phase (down triangles), $T_{\theta>0}$ phase (up triangles), and S phase (squares). We see that the actual U-$T_{\theta<0}$ phase boundary is well

described by the variational method, but one can notice a move of the S phase upwards and towards negative $\tilde{\mu}$. In fact, the vacuum-S-$T_{\theta>0}$ tricritical point moves to $\tilde{\mu} \approx -1.27$, $\gamma = 0.78$ (outside of the plot).

In Fig. 1 we also show density profiles corresponding to the points enclosed by rectangular frames in the phase diagram. The blue and yellow colors stand for minima and maxima of the density. Without this rescaling the contrast, for instance, in the lowest rightmost picture would be very weak. However, one can clearly distinguish smooth density profiles, which can be described by a few harmonics in the spirit of Eqs. (7) and (8), and sharper profiles (as one moves further away from the four-critical point) requiring more harmonics or a different *Ansatz*. The spatial coordinates have also been rescaled (except for the upper set in the violet frame) because the wave vector k_m changes very strongly from point to point.

To the right of the vacuum curve (empty circles in Fig. 1) the pressure is $P = -\Omega > 0$ and, therefore, this region of the phase diagram requires an external trapping. In Fig. 2 we present the exact GP result for an isotropically trapped gas with $g_2 < 0$, $\gamma = 0.575$, the global chemical potential $\tilde{\mu} = 0.6$, and trap frequency $\tilde{\omega} = 0.05$ (in units of $g_2^2/\hbar g_3$). The result is consistent with the local density approximation in which moving from the trap center towards its edge is equivalent to the trajectory along a horizontal line in Fig. 1 determined by the local chemical potential $\mu(r) = \mu - m\omega^2 r^2/2$. In Fig. 2 one can clearly distinguish the U phase in the trap center, the transition to the $T_{\theta<0}$ phase, and eventually to the S phase. As the local chemical potential decreases, the contrast and the period of the density modulation increase, which is consistent with the free space results.

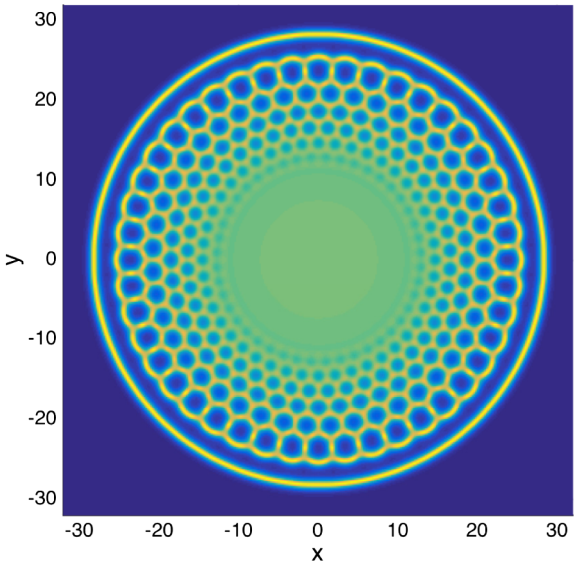

FIG. 2 (color online). The density profile for a harmonically trapped gas with $\tilde{\mu} = 0.6$, $\gamma = 0.575$, and trapping frequency $\tilde{\omega} = 0.05$. The coordinates x, y are in units of $\sqrt{\hbar^2 g_3/m g_2^2}$.

We should point out that first-order transitions involving density jumps are forbidden in 2D systems with dipolar interaction tails. The reason is that the surface tension in between two such phases can have a negative contribution, which logarithmically diverges with the length of the interface and can thus overcome the positive local scale-independent contribution [45] (see also Ref. [20]). This means that the first-order transition curves that we describe here become (narrow) regions of intermediate "microemulsion" phases [45]. It is argued [20,46] that the observation of these phases requires exponentially large system sizes, which are likely much larger than the size of a typical ultracold sample. Nevertheless, we note that already the simplest vacuum-U interface that we predict in our dilute weakly interacting system should be a good candidate for studying these interfacial effects. However, we leave this subject for future work.

In conclusion, we have found that a dilute 2D dipolar Bose gas can reside in a variety of supersolid phases stabilized by three-body repulsion. Our results represent a starting point for the analysis of collective modes of homogeneous, trapped or self-trapped supersolids. The developed approach can also be employed in the studies of novel vortex and soliton structures, and in the search for translationally nonperiodic phases, in particular, density-disordered superfluid (superglass) phases.

Promising candidates for the creation of such dipolar Bose gases are (nonreactive) polar molecules in the bilayer geometry with interlayer tunneling. The validity of the Hamiltonian (1) requires the tunneling amplitude t be much larger than the interaction energy per particle (chemical potential). For the 2D confinement frequency $\sim$50 kHz and interlayer spacing $\lambda \approx 200$ nm one has $t \sim 100$ nK for nonreactive NaK molecules. In the region of stability of supersolid states in the phase diagram in Fig. 1 we have γ in between 0.3 and 0.85, so that for $r_* \sim \lambda$ one has the three-body coupling constant $g_3 \sim 2\pi^2\hbar^2\lambda^2/m$. The characteristic value of the chemical potential in the stability region is $|\mu| \sim g_2^2/g_3$ ($|\tilde{\mu}| \sim 1$) and it can be easily made about 10 nK, which is much smaller than t. The chemical potential is related to the 2D density as $\mu = g_2 n + g_3 n^2/2$, and for g_3 specified above the value $|\mu| \sim 10$ nK corresponds to $n \sim 5 \times 10^8$ cm^{-2}. Therefore, the Kosterlitz-Thouless critical temperature $T_{\mathrm{KT}} = \pi\hbar^2 n_s/2m$ (n_s is the superfluid density just below T_{KT} and in our conditions it is about a factor of 3 or 4 lower than the total density) will be $\sim$20 nK. Then, in analogy with spinor Bose gases (see Ref. [47]) for the supersolid-uniform difference in the interaction energy per particle of a few nanokelvins the system should Bose condense to the supersolid state in the region of its stability shown in Fig. 1. We thus see that the observation of dilute supersolid states proposed in this Letter is feasible at temperatures of a few tens of nanokelvins.

We acknowledge support from IFRAF and from the Dutch Foundation FOM. The research leading to these

results has received funding from the European Research Council under the European Community's Seventh Framework Programme (FR7/2007-2013 Grant Agreement No. 341197). Y. L. acknowledges support from the ARC Discovery Projects (Grants No. DE150101636 and No. DP140103231).

[1] K.-K. Ni, S. Ospelkaus, M. H. G. de Miranda, A. Pe'er, B. Neyenhuis, J. J. Zirbel, S. Kotochigova, P. S. Julienne, D. S. Jin, and J. Ye, Science **322**, 231(2008).
[2] See for review L. D. Carr, D. DeMille, R. V. Krems, and J. Ye, New J. Phys. **11**, 055049 (2009).
[3] M. Lu, N. Q. Burdick, S. H. Youn, and B. L. Lev, Phys. Rev. Lett. **107**, 190401 (2011).
[4] K. Aikawa, A. Frisch, M. Mark, S. Baier, A. Rietzler, R. Grimm, and F. Ferlaino, Phys. Rev. Lett. **108**, 210401 (2012).
[5] S. Ospelkaus, K.-K. Ni, D. Wang, M. H. G. de Miranda, B. Neyenhuis, G. Quemener, P. S. Julienne, J. L. Bohn, D. S. Jin, and J. Ye, Science **327**, 853 (2010).
[6] K.-K. Ni, S. Ospelkaus, D. Wang, G. Quéméner, B. Neyenhuis, M. H. G. de Miranda, J. L. Bohn, J. Ye, and D. S. Jin, Nature (London) **464**, 1324 (2010).
[7] G. Quéméner and J. L. Bohn, Phys. Rev. A **81**, 060701 (2010).
[8] A. Micheli, Z. Idziaszek, G. Pupillo, M. A. Baranov, P. Zoller, and P. S. Julienne, Phys. Rev. Lett. **105**, 073202 (2010).
[9] M. H. G. de Miranda, A. Chotia, B. Neyenhuis, D. Wang, G. Quemener, S. Ospelkaus, J. L. Bohn, J. Ye, and D. S. Jin, Nat. Phys. **7**, 502 (2011).
[10] M. A. Baranov, Phys. Rep. **464**, 71 (2008).
[11] M. A. Baranov, M. Dalmonte, G. Pupillo, and P. Zoller, Chem. Rev. **112**, 5012 (2012).
[12] R. M. Wilson, C. Ticknor, J. L. Bohn, and E. Timmermans, Phys. Rev. A **86**, 033606 (2012).
[13] S. Gopalakrishnan, I. Martin, and E. A. Demler, Phys. Rev. Lett. **111**, 185304 (2013).
[14] C.-H. Wu, J. W. Park, P. Ahmadi, S. Will, and M. W. Zwierlein, Phys. Rev. Lett. **109**, 085301 (2012).
[15] J. W. Park, S. A. Will, and M. W. Zwierlein, Phys. Rev. Lett. **114**, 205302 (2015).
[16] T. Takekoshi, L. Reichsollner, A. Schindewolf, J. M. Hutson, C. R. Le Sueur, O. Dulieu, F. Ferlaino, R. Grimm, and H.-C. Nägerl, Phys. Rev. Lett. **113**, 205301 (2014).
[17] P. K. Molony, P. D. Gregory, Z. Ji, B. Lu, M. P. Köppinger, C. R. Le Sueur, C. L. Blackley, J. M. Hutson, and S. L. Cornish, Phys. Rev. Lett. **113**, 255301 (2014).
[18] E. P. Gross, Phys. Rev. **106**, 161 (1957); Ann. Phys. (N.Y.) **4**, 57 (1958).
[19] D. A. Kirzhnits and Yu. A. Nepomnyashchii, Sov. Phys. JETP **32**, 1191 (1971).
[20] A. B. Kuklov, N. V. Prokof'ev, and B. V. Svistunov, Physics **4**, 109 (2011); M. Boninsegni and N. V. Prokof'ev, Rev. Mod. Phys. **84**, 759 (2012).
[21] S. Balibar, Nature (London) **464**, 176 (2010).
[22] Here, we focus on continuous space supersolids.
[23] Y. Pomeau and S. Rica, Phys. Rev. Lett. **72**, 2426 (1994).
[24] N. Henkel, R. Nath, and T. Pohl, Phys. Rev. Lett. **104**, 195302 (2010).
[25] F. Cinti, P. Jain, M. Boninsegni, A. Micheli, P. Zoller, and G. Pupillo, Phys. Rev. Lett. **105**, 135301 (2010).
[26] S. Saccani, S. Moroni, and M. Boninsegni, Phys. Rev. B **83**, 092506 (2011).
[27] I. L. Kurbakov, Yu. E. Lozovik, G. E. Astrakharchik, and J. Boronat, Phys. Rev. B **82**, 014508 (2010).
[28] H. P. Buchler, E. Demler, M. Lukin, A. Micheli, N. Prokof'ev, G. Pupillo, and P. Zoller, Phys. Rev. Lett. **98**, 060404 (2007).
[29] G. E. Astrakharchik, J. Boronat, I. L. Kurbakov, and Yu. E. Lozovik, Phys. Rev. Lett. **98**, 060405 (2007).
[30] L. Santos, G. V. Shlyapnikov, and M. Lewenstein, Phys. Rev. Lett. **90**, 250403 (2003).
[31] G. V. Shlyapnikov and P. Pedri, Conference on Correlated and Many-Body Phenomena in Dipolar Systems, Max Planck Institute for Complex systems, Dresden, 2006 (2006).
[32] S. Komineas and N. R. Cooper, Phys. Rev. A **75**, 023623 (2007).
[33] H.-W. Hammer, A. Nogga, and A. Schwenk, Rev. Mod. Phys. **85**, 197 (2013).
[34] D. S. Petrov, Phys. Rev. Lett. **112**, 103201 (2014).
[35] A. Boudjemaa and G. V. Shlyapnikov, Phys. Rev. A **87**, 025601 (2013).
[36] L. P. Pitaevskii, JETP Lett. **39**, 511 (1984).
[37] P. Nozieres, J. Low Temp. Phys. **137**, 45 (2004); **142**, 91 (2006); **156**, 9 (2009).
[38] See Supplemental Material at http://link.aps.org/supplemental/10.1103/PhysRevLett.115.075303, which includes Ref. [39,40], for details of our numerical procedure and explicit expressions for $\mathcal{D}_{T(S)}(\theta)$, $\mathcal{C}_{T(S)}(\theta)$, and $\mathcal{T}_{T(S)}(\theta)$.
[39] W. H. Press, S. A. Teukolsky, W. T. Vetterling, and B. P. Flannery, *Numerical Recipes*, 3rd ed. (Cambridge University Press, Cambridge, England, 2007).
[40] K. Góral and L. Santos, Phys. Rev. A **66**, 023613 (2002).
[41] L. D. Landau and E. M. Lifshitz, *Statistical Physics, Part 1* (Pergamon Press, New York, 1969).
[42] K. Binder, Rep. Prog. Phys. **50**, 783 (1987).
[43] In fact, one can think of the $g_2 = 0$ case as being represented by a vertical line in Fig. 1 drawn at infinite $\tilde{\mu}$.
[44] Such droplets have been discussed for 3D Bose condensates with contact two- and three-body interactions by A. Bulgac, Phys. Rev. Lett. **89**, 050402 (2002).
[45] B. Spivak and S. A. Kivelson, Phys. Rev. B **70**, 155114 (2004).
[46] S. Moroni and M. Boninsegni, Phys. Rev. Lett. **113**, 240407 (2014).
[47] D. M. Stamper-Kurn and M. Ueda, Rev. Mod. Phys. **85**, 1191 (2013).